Kinetics and Mechanism of the IO + BrO Reaction

Yuri Bedjanian,* Georges Le Bras, and Gilles Poulet

Laboratoire de Combustion et Systèmes Réactifs, CNRS and Université d'Orléans, 45071 Orléans Cedex 2, France

Received: July 10, 1998; In Final Form: October 7, 1998

The kinetics and mechanism of reaction 1 between IO and BrO radicals have been studied by the mass spectrometric discharge flow method at 298 K. The value of the overall rate constant $k_1 = (8.5 \pm 1.5) \times 10^{-11}$ cm^3 molecule^{-1} s^{-1} has been determined from the simultaneous monitoring of BrO and IO. The branching ratios have been measured for the various channels of reaction 1 in different series of experiments. The branching ratio for the major channel, producing Br and OIO, has been found in the range 0.65−1.0. The upper limits of the branching ratios for the channels producing I + Br + O_2, I + OBrO, and IBr + O_2 are 0.3, 0.2, and 0.05, respectively, whereas an upper limit of 0.3 has been found for the sum of the branching ratios for the I-atom-producing channels. Rate coefficients for side reactions have been also redetermined under the conditions of the present study: BrO + BrO → products, I + O_3 → IO + O_2, NO + O_3 → NO_2 + O_2, Br + IO → I + BrO, BrO + I_2 → products, and BrO + IBr → products. The kinetic data obtained for the IO + BrO reaction allow one to derive an upper limit for the enthalpy of formation of OIO: $\Delta H°_{f,298}$ (OIO) ≤ 32.2 kcal mol^{-1}. The atmospheric implications of the present data are briefly discussed.

Introduction

It has been known for a long time that halogenated compounds are strongly involved in stratospheric ozone chemistry. Mostly chlorine and bromine chemistry have been investigated, both in the field and in the laboratory. The role of iodine has already been considered in relation to tropospheric chemistry, particularly in the marine boundary layer (e.g., refs 1 and 2) and in the Arctic troposphere during ozone depletion events observed in recent years.[3,4] Although iodine is known to be released from the oceans, essentially as CH_3I, the magnitude of this marine source is still uncertain.[5] As suggested by Solomon et al.,[6] the iodine-containing species, which have short lifetimes, can only reach the lower stratosphere if an efficient convective transport exists, which may be the case in the tropics. Very recent observations disagree on the abundance of stratospheric iodine, ranging from an upper limit of 0.1 ppt[7,8] to 0.5 ppt in the tropical stratosphere.[5] In addition to atmospheric measurements of the iodine abundance, the potential role of iodine in ozone chemistry requires a better knowledge of the kinetic and mechanistic parameters of the reactions of the IO radical, which plays a key role in this chemistry.

It is now accepted that, in the reaction sequence which might lead to ozone loss, initiated by IO, iodine may participate only by interacting either with HO_2 or with XO radicals, where X denotes Cl and Br. In the latter case, the catalytic cycle reaction is

$$\mathrm{IO + XO \rightarrow products}$$

This reaction must be very fast and lead to the production of halogen atoms (I and X) to produce an ozone loss cycle. Therefore, to quantify the ozone depletion resulting from the potential presence of iodine in the stratosphere, both kinetic and mechanistic data are required for these interhalogen radical−radical reactions. The IO + ClO reaction has been studied in detail recently, in two laboratories, including this one.[9,10] Kinetic data on the IO + BrO reaction have also been published very recently.[11,12] In one of these studies,[11] the overall rate constant of the IO + BrO reaction has been derived from the modeling analysis of a complex reaction system. In the other study,[12] the rate constant has been measured only for the non-iodine-atom-producing channels. Because the IO + BrO reaction may proceed via several channels, it was concluded in this paper[12] that "the branching ratios for various channels are still unclear and need to be explored". The present study aims at clarifying the mechanism of this IO + BrO reaction, for which the thermochemically feasible channels are:

$$\mathrm{IO + BrO \rightarrow Br + OIO} \qquad \Delta H \le 0 \text{ kcal mol}^{-1} \quad (1a)$$

$$\rightarrow \mathrm{Br + I + O_2} \qquad \Delta H = -4.1 \pm 2.6 \text{ kcal mol}^{-1} \quad (1b)$$

$$\rightarrow \mathrm{I + OBrO} \qquad \Delta H = 5.5 \pm 8.6 \text{ kcal mol}^{-1} \quad (1c)$$

$$\rightarrow \mathrm{IBr + O_2} \qquad \Delta H = -46.5 \pm 2.6 \text{ kcal mol}^{-1} \quad (1d)$$

The thermochemical data used for the calculations of ΔH are from references 13 (I, Br), 14 and 15 (IBr), 9 (IO), 16 (BrO), and 17 (OBrO). The enthalpy of channel 1a has been estimated from the present study. Channel 1b can be written as a two-step reaction, the primary products being either IOO + Br or BrOO + I.

Experimental Section

All experiments have been carried out at $T = 298$ K and at a total pressure of 1 Torr of helium. The experiments have been carried out using a molecular beam mass spectrometer coupled to a discharge flow system, as described previously (e.g., ref 9). The reactor consisted of a Pyrex tube (45 cm length and 2.4

10.1021/jp982972n CCC: $15.00
Published on Web 12/02/1998

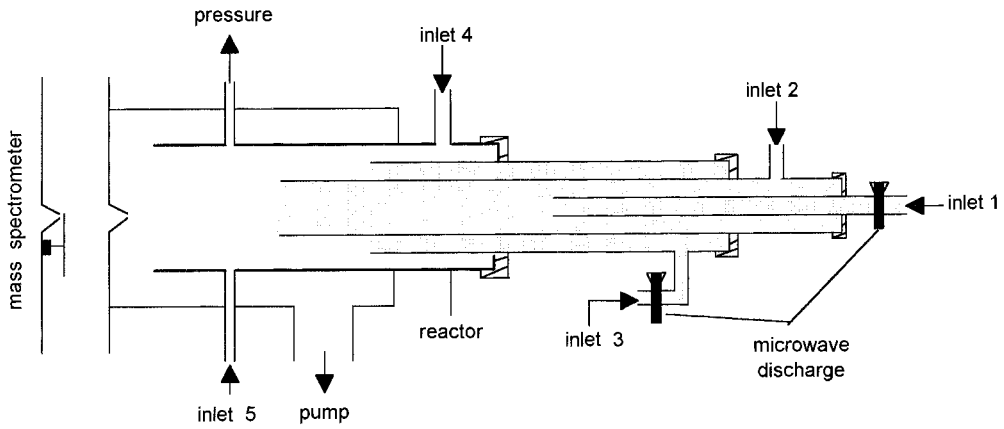

Figure 1. Diagram of the apparatus used.

cm i.d.), and a triple movable injector was used to introduce the reactants into the reactor (Figure 1). To reduce the heterogeneous loss of the active species, the surfaces of the main reactor and of the injector were coated with halocarbon wax.

Three different methods were used for the production of IO radicals: the reaction of oxygen atoms (formed in a microwave discharge of O_2/He mixtures) with molecular iodine or trifluoromethyl iodide

$$O + I_2 \rightarrow IO + I$$
$$k_2 = 1.4 \times 10^{-10}\ \text{cm}^3\,\text{molecule}^{-1}\,\text{s}^{-1}\ ^{13} \quad (2)$$

$$O + CF_3I \rightarrow IO + CF_3$$
$$k_3 = 3.65 \times 10^{-12}\ \text{cm}^3\,\text{molecule}^{-1}\,\text{s}^{-1}\ ^{18} \quad (3)$$

and the reaction of iodine atoms with ozone

$$I + O_3 \rightarrow IO + O_2 \quad k_4 = 1.2 \times 10^{-12}\ \text{cm}^3\,\text{molecule}^{-1}\,\text{s}^{-1}\ ^{13} \quad (4)$$

(all rate constants are given at 298 K).

In the latter source, I atoms were produced from the reaction

$$Br + I_2 \rightarrow I + IBr \quad k_5 = 1.2 \times 10^{-10}\ \text{cm}^3\,\text{molecule}^{-1}\,\text{s}^{-1}\ ^{16} \quad (5)$$

An excess either of I_2 over Br or of Br over I_2 was used, depending on the objective of the experiments. Br atoms were generated in a microwave discharge of Br_2/He mixtures. Molecular iodine was introduced into the reactor by flowing helium through a column containing I_2 crystals. The concentration of IO radicals was determined using titration with NO

$$IO + NO \rightarrow I + NO_2$$
$$k_6 = 2.0 \times 10^{-11}\ \text{cm}^3\,\text{molecule}^{-1}\,\text{s}^{-1}\ ^{13} \quad (6)$$

with the subsequent mass spectrometric detection of the NO_2 formed and calibration of the mass spectrometer by flowing known concentrations of NO_2 into the reactor. Calibration experiments were carried out under conditions when the possible influence of the self-combination and/or heterogeneous loss of IO was negligible:

$$IO + IO \rightarrow \text{products}$$
$$k_7 = 8.0 \times 10^{-11}\ \text{cm}^3\,\text{molecule}^{-1}\,\text{s}^{-1}\ ^{13} \quad (7)$$

$$IO + \text{wall} \rightarrow \text{products} \quad k_w = 20-40\ \text{s}^{-1}\ \text{(this work)}$$

With an excess of molecular iodine over Br atoms, reaction 5 was used for the determination of the absolute concentrations of I atoms and of I_2 and IBr molecules: $[Br]_0 = \Delta[I_2] = [I] = [IBr]$. The absolute concentrations of Br atoms were determined from the measurements of the fraction of Br_2 dissociated in the microwave discharge: $[Br]_0 = 2\Delta[Br_2]$. To verify the ratio of the intensities of the mass spectrometric signals of I and IBr corresponding to the same concentration, additional runs were performed using the titration of IBr with an excess of Br via reaction 8 leading to $[IBr]_0 = [I]$:

$$Br + IBr \rightarrow I + Br_2$$
$$k_8 = 2.7 \times 10^{-11}\ \text{cm}^3\,\text{molecule}^{-1}\,\text{s}^{-1}\ ^{15} \quad (8)$$

The same procedure was applied for I_2 and I, using the titration of molecular iodine with an excess of Br atoms in reaction 5, followed by the titration of IBr produced, using reaction 8, which led to $[I_2]_0 = 2[I]$. The results of these relative calibrations agreed very well (within 10%) with the absolute ones.

Two sources of BrO radicals were used:

$$O + Br_2 \rightarrow BrO + Br$$
$$k_9 = 1.4 \times 10^{-11}\ \text{cm}^3\,\text{molecule}^{-1}\,\text{s}^{-1}\ ^{19} \quad (9)$$

$$Br + O_3 \rightarrow BrO + O_2$$
$$k_{10} = 1.2 \times 10^{-12}\ \text{cm}^3\,\text{molecule}^{-1}\,\text{s}^{-1}\ ^{13} \quad (10)$$

Both the reaction of Br with ozone (10) ($[BrO] = [Br]_0 = 2\Delta[Br_2]$) and the reaction of BrO with NO (11) were used for the determination of the absolute concentrations of BrO radicals:

$$BrO + NO \rightarrow Br + NO_2$$
$$k_{11} = 2.1 \times 10^{-11}\ \text{cm}^3\,\text{molecule}^{-1}\,\text{s}^{-1}\ ^{13} \quad (11)$$

The results obtained by using both methods were in good agreement (within 10%). Besides, the ratio of mass spectrometric signals corresponding to the same concentrations of BrO and IO was measured in experiments, by using the conversion of low concentration of O atoms (to make negligible the IO + IO reaction) to BrO (reaction with an excess of Br_2) or to IO (reaction with an excess of I_2). The results from this relative calibration method agreed within 10% with the absolute ones.

Ozone was produced by an ozonizer (Trailigaz) and was collected and stored in a trap containing silica gel at $T = 195$ K. The trap was pumped before use to reduce the O_2 concentration. The resulting oxygen concentration was always <20% of the ozone concentration introduced into the reactor. The absolute

TABLE 1: Reaction BrO + BrO → Products (13): Experimental Conditions and Results

$[BrO]_0$ (10^{13} molecule cm^{-3})	k_{13} (10^{-12} cm^3 $molecule^{-1}$ s^{-1})	k_{13b} (10^{-13} cm^3 $molecule^{-1}$ s^{-1})
0.19	2.85	
0.19	2.75	
0.20	2.71	
0.29	2.64	
0.30	2.66	
0.39	2.61	
0.39	2.82	
0.41	2.65	
0.56	2.66	
0.57	2.78	
0.68	2.83	
0.78	2.84	
0.80		3.91
0.81	2.81	
0.90	2.64	
0.95	2.83	
1.16	2.69	
1.40		4.14
2.10		4.04
2.60		4.06
3.60		4.00
5.60		3.90

concentrations of O_3 were derived using the reaction of ozone with NO with detection and calibration of NO_2 formed ($\Delta[O_3] = \Delta[NO_2]$):

$$NO + O_3 \rightarrow NO_2 + O_2$$
$$k_{12} = 1.8 \times 10^{-14}\ cm^3\ molecule^{-1} s^{-1}\ ^{13} \quad (12)$$

All relevant species were detected by mass spectrometry at their parent peaks.

The purities of the gases used were as follows: He > 99.9995% (Alphagaz), passed through a liquid nitrogen trap before use; O_2 > 99.995% (Alphagaz); Br_2 > 99.99% (Aldrich); I_2 > 99.999% (Aldrich); IBr, 98% (Aldrich); CF_3I > 99% (Fluorochem); NO > 99% (Alphagaz), purified by trap-to-trap distillation to remove traces of NO_2; NO_2 > 99% (Alphagaz).

Results

Accurate measurement of the absolute concentrations of the labile species is very important because this is the main source of uncertainty in kinetic studies of such radical−radical reactions (in the determination of both the rate constant and the branching ratios for different channels). In this work, to verify the procedure used for the calibration of the mass spectrometric signals of BrO, Br, IO, I, and O_3, independent studies of well-known reactions have been performed: BrO + BrO, I + O_3, and NO + O_3. These reactions as well as the reactions Br + IO, BrO + I_2, and BrO + IBr were also important in the study of the BrO + IO reaction (see below).

Reaction BrO + BrO → Products (13). Four series of experiments were carried out to study the BrO self-reaction:

$$BrO + BrO \rightarrow Br + Br + O_2 \quad (13a)$$
$$\rightarrow Br_2 + O_2 \quad (13b)$$

In the first one, the overall rate constant of the reaction, $k_{13} = k_{13a} + k_{13b}$, was measured. BrO radicals were formed directly in the reactor from the rapid consumption of oxygen atoms (introduced through inlet 1 of the movable injector) by Br_2 (inlet 4) in reaction 9. The Br_2 concentration was (1.0−1.5) × 10^{14} molecule cm^{-3}, and the linear flow velocity was in the range 630−700 cm s^{-1}. After a rapid formation of BrO radicals, second-order decay kinetics due to reaction 13 were observed. The rate of heterogeneous BrO loss was very low (k_w < 0.5 s^{-1}) compared with the BrO self-reaction rate, so that its contribution to the BrO decay could be neglected. The BrO initial concentrations used as well as the results obtained for k_{13} are shown in Table 1. The mean value of k_{13} from Table 1 is (2.74 ± 0.09) × 10^{-12} cm^3 $molecule^{-1}$ s^{-1}. Finally, if 10% for systematic error is included, the recommended value at 298K is

$$k_{13} = (2.75 \pm 0.35) \times 10^{-12}\ cm^3\ molecule^{-1}\ s^{-1}$$

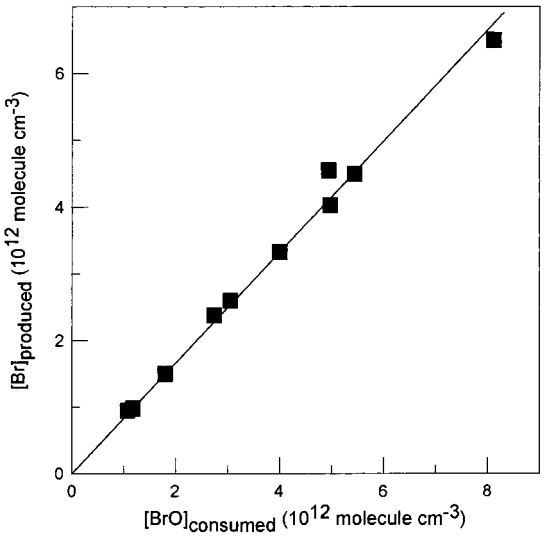

Figure 2. Reaction BrO + BrO → Br + Br + O_2 (13a): concentration of Br produced as a function of the concentration of BrO consumed.

Under the same experimental conditions, the Br atom formation in reaction 13 was observed and its yield was measured. For a fixed reaction time ($t \approx 0.04$ s), the consumed [BrO] and the corresponding concentration of Br atoms formed were measured. The initial concentration of BrO radicals was varied in the range (1.1−8.1) × 10^{12} molecule cm^{-3}. The results are shown in Figure 2, where the produced Br concentration is plotted as a function of the consumed BrO concentration. The slope of the line provides the value of the branching ratio for channel 13a, where the error is 1σ:

$$k_{13a}/k_{13} = \Delta[Br]/\Delta[BrO] = 0.84 \pm 0.03$$

The measurements of the rate constant for channel 13b were conducted in the presence of high ozone concentration: $[O_3]$ = (4.0−4.5) × 10^{15} molecule cm^{-3}. Under these conditions, Br atoms formed in channel 13a were rapidly converted back to BrO by reaction 10 and, as a result, channel 13a did not contribute to BrO consumption. The data derived from the BrO first-order decay kinetics are given in Table 1. The mean value of the six measurements of k_{13b} is (4.01 ± 0.09) × 10^{-13} cm^3 $molecule^{-1}$ s^{-1} (with statistical error only). Finally, if an additional 10% of uncertainty for the precision of BrO concentration measurements is included, the value of k_{13b} is

$$k_{13b} = (4.0 \pm 0.5) \times 10^{-13}\ cm^3\ molecule^{-1}\ s^{-1}$$

Using both values obtained for k_{13} and k_{13b}, the branching ratio for channel 13b can be derived, at 298 K

$$k_{13b}/k_{13} = 0.15 \pm 0.01$$

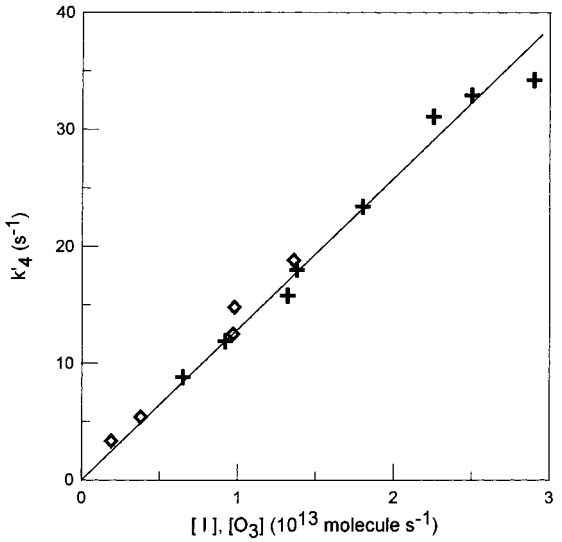

Figure 3. Reaction I + O_3 (4): pseudo-first-order plots obtained from the monitoring of O_3 consumption kinetics in excess of I atoms (+) and from IO formation kinetics (◇).

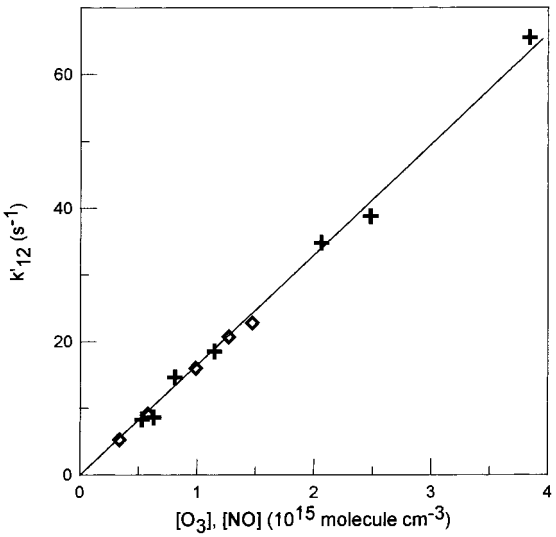

Figure 4. Reaction NO + O_3 (12): pseudo-first-order plots obtained from the monitoring of NO (+) and O_3 (◇) decay kinetics in excess of O_3 and NO, respectively.

The given uncertainty is the combination of statistical errors on k_{13} and k_{13b} only, because the k_{13b}/k_{13} ratio does not depend on a possible systematic error on the BrO absolute concentration measurements. The measurement of this ratio appears to be more accurate than that of k_{13a}/k_{13}, although both measurements of the ratios k_{13a}/k_{13} and k_{13b}/k_{13} are in excellent agreement.

In experiments using an excess of O_3, the formation of Br_2 in reaction 13b was also observed. In seven experiments the ratio $\Delta[BrO]/\Delta[Br_2]$ was derived from the measurement of BrO consumed and Br_2 produced:

$$\Delta[BrO]/\Delta[Br_2] = 1.9 \pm 0.15$$

The value obtained agrees well with the formation of one Br_2 molecule for two BrO radicals consumed in channel 13b and also confirms the validity of the procedure used for the absolute concentration measurements.

Finally, the present data for the BrO + BrO reaction at 298 K, $k_{13} = (2.75 \pm 0.35) \times 10^{-12}$ cm^3 molecule^{-1} s^{-1}, $k_{13b} = (4.0 \pm 0.5) \times 10^{-13}$ cm^3 molecule^{-1} s^{-1}, and $k_{13b}/k_{13} = 0.15 \pm 0.01$, are in good agreement with those recommended in the most recent evaluations:[13,20] $k_{13} = (3.2 \pm 0.5) \times 10^{-12}$ cm^3 molecule^{-1} s^{-1} and $k_{13b}/k_{13} = 0.15 \pm 0.03$[13]; and $k_{13} = (2.5 \pm 0.25) \times 10^{-12}$, $k_{13b} = (3.8 \pm 0.4) \times 10^{-13}$ cm^3 molecule^{-1} s^{-1}.[20]

Reaction I + O_3 → IO + O_2 (4). This reaction was studied in two series of experiments. In the first one, the kinetics of ozone consumption were monitored in the presence of an excess of I atoms. The initial concentration of O_3 was $\sim 7 \times 10^{11}$ molecule cm^{-3}, the concentration of I was varied in the range $(0.65-2.9) \times 10^{13}$ molecule cm^{-3}, and the flow velocity in the reactor was 750−800 cm s^{-1}. O_3 was introduced through the central injector (inlet 1). Iodine atoms were formed by reaction 5 using an excess of I_2 ($[I_2]_0 \approx 10^{14}$ molecule cm^{-3}), Br_2 and I_2 being introduced through inlets 3 and 4, respectively. The results obtained are given in Figure 3, which shows the dependence of the pseudo-first-order rate constant ($k'_4 = k_4[I]$) on the iodine atom concentration. It should be noted that some consumption of I was observed (up to 30% in some kinetic runs), which was attributed to heterogeneous loss, and the mean I concentration along the reaction zone was used in the calculations of k_4.

In a second series of experiments, the kinetics of IO formation in reaction 4 were also observed. These experiments were carried out with a fixed concentration of I atoms ($\sim 2 \times 10^{12}$ molecule cm^{-3}), with O_3 concentration in the range $(0.19-1.36) \times 10^{13}$ molecule cm^{-3} and a mean flow velocity of 1500 cm s^{-1}. Under these conditions, only a few percent of the initial concentration of I atoms was consumed. The concentration of IO formed was low enough ($<10^{11}$ molecule cm^{-3}) that the IO loss rate due to self-reaction and reaction with the wall ($k_w \approx 20$ s^{-1}) was negligible compared with the rate of IO formation in reaction 4. Consequently, linear kinetics of IO formation were observed according to

$$d[IO]/dt = k_4[I][O_3]$$

where [I] and $[O_3]$ could be considered as constant. The results thus obtained are also given in Figure 3, which shows the dependence of $k'_4 = (1/[I]) \times (d[IO]/dt)$ on the ozone concentration. As one can see, the data obtained by using the two different methods are in good agreement. The value of the rate constant for reaction 4, derived from all experimental data, is

$$k_4 = (1.3 \pm 0.25) \times 10^{-12} \text{ cm}^3 \text{ molecule}^{-1} \text{ s}^{-1}$$

(the error represents one standard deviation with addition of 15% uncertainty for the measurements of IO concentration). This value well agrees with the current recommendations: $k_4 = (1.2 \pm 0.2) \times 10^{-12}$ [13] and $(1.0 \pm 0.2) \times 10^{-12}$ cm^3 molecule^{-1} s^{-1} [20]. The good agreement between the two methods used in the present work for the determination of k_4 also indicates the reliability of the procedure used for the absolute calibration of the species involved in this study, particularly for the IO radicals, for which low concentrations are required in the subsequent experiments.

Reaction NO + O_3 → NO_2 + O_2 (12). The rate constant of reaction 12 was measured in two sets of experiments under pseudo-first-order conditions, using either an excess of ozone ($[O_3] = (0.5-3.8) \times 10^{15}$ molecule cm^{-3}) over NO ($[NO]_0 \approx 10^{12}$ molecule cm^{-3}) and monitoring the NO decay kinetics or an excess of NO ($[NO] = (0.4-1.5) \times 10^{15}$, $[O_3] \approx 10^{12}$ molecule cm^{-3}) and monitoring the O_3 consumption kinetics. The flow rate in the reactor was 440−550 cm s^{-1}. The pseudo-first-order plots thus obtained are shown in Figure 4. The results of these two series of experiments are in good agreement, and

the value of the rate constant k_{12} derived using all experimental data is

$$k_{12} = (1.65 \pm 0.20) \times 10^{-14}\ \text{cm}^3\ \text{molecule}^{-1}\ \text{s}^{-1}$$

where the uncertainty represents one standard deviation with addition of 10% for possible systematic error. The formation of NO_2 was observed in both series of experiments, and the relation $\Delta[NO_2] = \Delta[NO] = \Delta[O_3]$ was verified to hold within 10%. The present value of k_{12} also agrees with the current recommendations: $k_{12} = (1.8 \pm 0.20) \times 10^{-14}$ cm^3 molecule^{-1} s^{-1}.[13,20]

Reaction Br + IO → I + BrO (14). Reaction 14 is of importance for the IO + BrO reaction study as it can be a secondary or side process. The rate constant of this reaction has been measured in two previous studies:[16,21] at room temperature, $k_{14} = (2.3 \pm 0.3) \times 10^{-11}$ [16] and $(5.0 \pm 1.1) \times 10^{-11}$ cm^3 molecule^{-1}s^{-1}.[21] One of these studies[16] is from this laboratory, and k_{14} was measured under pseudo-first-order conditions, using an excess of Br atoms over IO radicals. Two sources of Br atoms were used: dissociation of Br_2 in a microwave discharge and reaction of Cl atoms with C_2H_3Br. The same experiments have been repeated here using two different methods for Br detection: direct detection at the parent peaks $m/e = 79$ and 81 (Br^+) and indirect detection at $m/e = 116$ ($BrCl^+$), after Br conversion into BrCl in reaction 15, ClNO being introduced at the downstream end of the reactor (through inlet 5):

$$\text{Br} + \text{ClNO} \rightarrow \text{BrCl} + \text{NO} \qquad k_{15} = 1.25 \times 10^{-11}\ \text{cm}^3\ \text{molecule}^{-1}\ \text{s}^{-1}\ [22] \quad (15)$$

This method of Br detection was free of complications arising from the contributions of Br_2 and/or BrO at $m/e = 79$ and 81 due to their dissociation−ionization in the ion source of the mass spectrometer. IO radicals were generated by reaction 3 between O atoms (inlet 3) and CF_3I, at concentrations of $\sim 10^{14}$ molecule cm^{-3} (inlet 4). Br atoms were produced in the microwave discharge of Br_2/He mixtures and introduced into the reactor through the internal tube of the movable injector. The following experimental conditions were used: $[IO]_0 = (5-7) \times 10^{10}$, $[Br]_0 = (0.05-2.4) \times 10^{13}$ molecule cm^{-3}, and linear flow velocity = 1550 cm s^{-1}. The pseudo-first-order plot obtained from the IO decay kinetics is shown in Figure 5. All of the measured values of k'_{14} were corrected for axial and radial diffusion[23] of IO. The diffusion coefficient $D_{\text{IO-He}} = 410$ cm^2 s^{-1} (1 Torr) was calculated from $D_{\text{Xe-He}}$.[24] The correction was <10%. The results obtained with the two methods used for Br detection are in good agreement and yield the following value of k_{14}:

$$k_{14} = (2.7 \pm 0.4) \times 10^{-11}\ \text{cm}^3\ \text{molecule}^{-1}\ \text{s}^{-1}$$

(the error is 1σ + 10% uncertainty). The intercept of the plot of Figure 5 is 9.3 ± 11.5 s^{-1}, which is in good agreement with the IO decay rate, 18 ± 5 s^{-1}, measured separately in the absence of Br atoms.

The presence of I atoms coming from the IO source, possibly formed in the secondary reactions O + IO and IO + IO, may lead to the underestimation of k_{14} due to IO formation in the reverse reaction (−14):

$$\text{I} + \text{BrO} \rightarrow \text{IO} + \text{Br} \qquad k_{-14} = 1.45 \times 10^{-11}\ \text{cm}^3\ \text{molecule}^{-1}\ \text{s}^{-1}\ [16] \quad (-14)$$

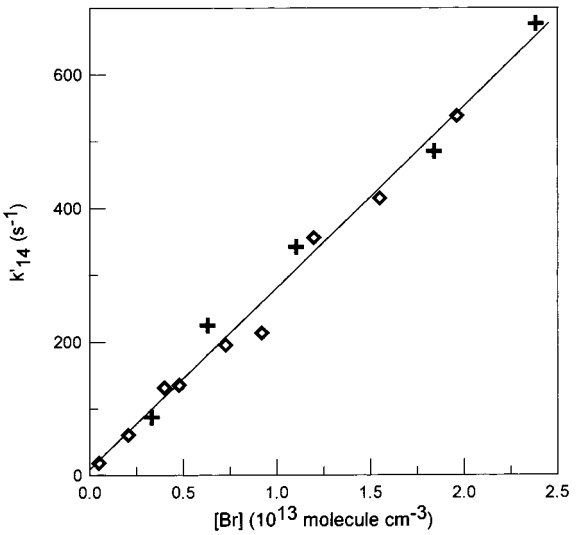

Figure 5. Reaction Br + IO (14): pseudo-first-order plots obtained from the monitoring of IO consumption kinetics in excess of Br atoms, with Br detected at m/e 79/81 (+) and at $m/e = 116$ (◇) as BrCl (see text).

To estimate this residual concentration of I atom, ozone was added at the downstream end of the reactor (after completion of the O + CF_3I reaction) to convert I atoms into IO. From the measured increase of the IO signal, it was calculated that this concentration of I atoms was always <20% of that of initial IO. That indicates that the occurrence of reaction −14 has a negligible effect on the results obtained for k_{14}, due to the low concentration of both I and BrO. Finally, the mean value of our two measurements for k_{14} (ref16 and the present study) will be used in the study of the IO + BrO reaction, that is

$$k_{14} = (2.5 \pm 0.5) \times 10^{-11}\ \text{cm}^3\ \text{molecule}^{-1}\ \text{s}^{-1}$$

The origin for the discrepancy by a factor 2 between this value and the other one[21] is not clear. However, it can be noted that the data obtained for the IO + BrO reaction were not sensitive to this uncertainty.

Reactions of BrO with I_2 (16) and IBr (17). Kinetic data for the reactions of BrO radicals with the IO precursor, I_2, and with the possible product of reaction 1, IBr, were needed before studying the IO + BrO reaction:

$$\text{BrO} + \text{I}_2 \rightarrow \text{products} \quad (16)$$

$$\text{BrO} + \text{IBr} \rightarrow \text{products} \quad (17)$$

Experiments were carried out using an excess of the molecular species over BrO. Reaction 9 between O and Br_2 was used as the BrO source. An experimental complication appeared from the simultaneous Br formation in reaction 9, initiating the fast secondary chemistry:

$$\text{Br} + \text{I}_2 \rightarrow \text{I} + \text{IBr} \quad (5)$$

$$\text{I} + \text{BrO} \leftrightarrow \text{Br} + \text{IO} \quad (-14,14)$$

$$\text{IO} + \text{BrO} \rightarrow \text{products} \quad (1)$$

A similar complication appeared in the case of IBr. It was verified that the BrO consumption rate strongly depended on BrO and Br initial concentrations. However, the contribution of this secondary chemistry to BrO decay (for a given $[BrO]_0$) should be independent of $[I_2]_0$. If $[I_2]_0$ is large enough to ensure rapid consumption of Br in reaction 5, reaction 16 becomes the

limiting step. The initial concentration of BrO was kept low to minimize the contribution of secondary reactions ([BrO] = 3×10^{11} molecule cm^{-3}), whereas [I_2] and [IBr] were varied in the ranges $(0.4-2.4) \times 10^{14}$ and $(0.2-1.0) \times 10^{14}$ molecule cm^{-3}, respectively. The rate of BrO decay was observed to be independent of [I_2] (in the case of reaction 16) and of IBr (in the case of reaction 17) and was 15.2 ± 2.1 and 16.3 ± 1.0 s^{-1}, respectively. From these data, the upper limits of the values of the rate constants for reactions 16 and 17 were found to be, at 298 K:

$$k_{16} \leq 2 \times 10^{-14} \text{ cm}^3 \text{ molecule}^{-1} \text{ s}^{-1}$$

$$k_{17} \leq 2.5 \times 10^{-14} \text{ cm}^3 \text{ molecule}^{-1} \text{ s}^{-1}$$

Reaction 10 between Br and O_3 was not used as a source of BrO in these experiments, to avoid any possible BrO regeneration by the reaction of Br atoms (from primary and secondary steps) with ozone.

Reaction IO + BrO → Products (1). *(a) Rate Constant for Non-I-Atom-Producing Channels.* The kinetic study of reaction 1 was carried out under pseudo-first-order conditions, using an excess of BrO over IO: [BrO] = $(0.4-9.7) \times 10^{12}$, $[IO]_0 = (0.5-1.0) \times 10^{11}$ molecule cm^{-3}. Relatively high O_3 concentrations were present in the reactor [[O_3] = $(1.0-3.8) \times 10^{15}$ molecule cm^{-3}] to ensure a rapid transformation of I atoms, possibly formed in reaction 1, back to IO via reaction 4. Different configurations for the production of the reactants and their introduction into the reactor were used. In most experiments, IO and BrO radicals were formed directly in the reactor, from reactions of I and Br with O_3, respectively. I atoms were produced in the reaction of I_2 (or IBr) (inlet 2) with Br atoms in excess, formed in a microwave discharge of Br_2/He mixtures (inlet 1) in the movable injector:

$$\text{Br} + \text{I}_2 \rightarrow \text{I} + \text{IBr} \quad (5)$$

$$\text{Br} + \text{IBr} \rightarrow \text{I} + \text{Br}_2 \quad (8)$$

Thus produced, I and Br atoms were rapidly consumed in the reactor by the excess of ozone (inlet 4), forming IO and BrO radicals, respectively. Another configuration was used, in which O_3 was added through the central tube of the injector (inlet 1) and Br_2 and I_2 were added through inlets 3 and 4, respectively. Finally, a few experiments were carried out with separated production zones of BrO and IO: BrO was formed in the movable injector by the Br + O_3 reaction (Br, inlet 1; O_3, inlet 2) and IO by the reaction of O atoms with excess I_2 (O, inlet 3; I_2, inlet 4). In the latter case, the concentration used for I_2 was $\sim 10^{12}$ molecule cm^{-3}. The flow velocity in the reactor was in the range 1350−1550 cm s^{-1}. Under the experimental conditions used, the BrO decay, which was due to reaction 1, to BrO wall loss ($k_w \leq 0.05$ s^{-1}) and to the minor channel of the BrO self-reaction 3b was observed to be negligible. The data obtained from the IO exponential decay kinetics are shown in Figure 6. All values of the pseudo-first-order rate constant k'_1 were corrected for the axial and radial diffusion of IO radicals (correction always <10%). The straight line obtained in Figure 6 results from the linear least-squares fit to experimental data, and its slope gives the value of the rate constant for the non-I-atom-producing channels of reaction 1, that is, reactions 1a and 1d

$$k_{1a} + k_{1d} = (7.5 \pm 1.0) \times 10^{-11} \text{ cm}^3 \text{ molecule}^{-1} \text{ s}^{-1}$$

(the uncertainty represents $1\sigma + 10\%$). The value of the intercept

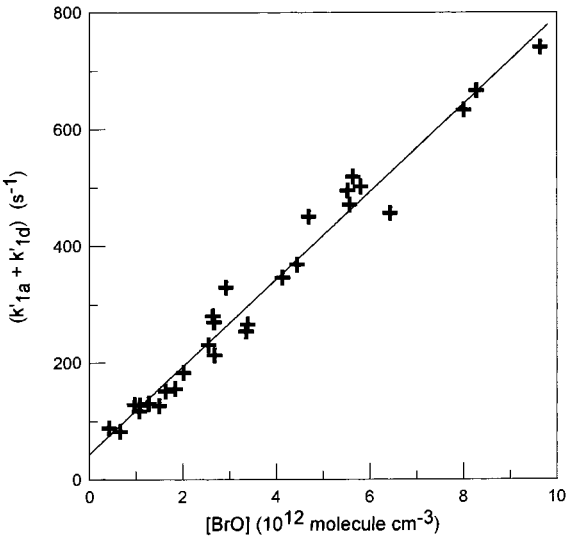

Figure 6. Reaction BrO + IO → products (1): pseudo-first-order plot of the IO consumption by the non-I-atom producing channels (see text).

TABLE 2: Reaction IO + BrO → Products (1): IO Kinetics in the Presence of Br[a]

reaction	no.	rate constant[b]	ref
O + CF_3I → IO + CF_3	3	3.7×10^{-12}	18
O + Br_2 → Br + BrO	9	1.4×10^{-11}	19
O + BrO → Br + O_2	18	4.1×10^{-11}	13
O + IO → I + O_2	19	1.2×10^{-10}	13
CF_3 + Br_2 → Br + CF_3Br	20	1.8×10^{-12}	26
IO + BrO → Br	1	variable	
IO + IO → products	7	8.0×10^{-11}	13
IO + wall → loss		30	this work
IO + Br → BrO + I	14	2.5×10^{-11}	16, this work
BrO + I → IO + Br	−14	1.5×10^{-11}	16
BrO + BrO → Br + Br + O_2	13a	2.35×10^{-12}	this work
BrO + BrO → Br_2 + O_2	13b	4.0×10^{-13}	this work
I + Br_2 → IBr + Br	−8	1.65×10^{-13}	15
Br + IBr → I + Br_2	8	2.7×10^{-11}	15

[a] Mechanism used for the modeling of the experimental profiles of IO, BrO, and Br. [b] Units are cm^3 molecule^{-1} s^{-1} for bimolecular reactions and s^{-1} for heterogeneous reaction.

(40 ± 22) s^{-1} includes the rates of the IO heterogeneous loss and the IO self-reaction. This value is in fair agreement with the IO decay rate measured in the absence of BrO: (20−40 s^{-1}) and is relatively low compared with the rate of reaction 1. No dependence of the obtained results on the concentration of O_3 (which was varied by a factor of 4) and on the sources used for the reactants was observed.

(b) IO Decay Kinetics in the Presence of Br. In this series of experiments, the kinetics of the IO + BrO reaction have been studied in the presence of Br atoms. Oxygen atoms formed in a microwave discharge of O_2/He mixtures (inlet 1) and introduced into the reactor through the central tube of the movable injector reacted with a mixture of CF_3I (inlet 4) and Br_2 (inlet 3), producing simultaneously IO radicals (reaction 3) and BrO and Br (reaction 9). The observed kinetics of IO, BrO, and Br were fitted using FACSIMILE[25] based on the mechanism given in Table 2. Typical concentration−time profiles (measured and calculated) are shown in Figure 7. The experimental conditions used are summarized in Table 3. The initial concentrations of O atoms were determined from the measurements of the dissociated fraction of known concentration of O_2 in the microwave discharge. At relatively low [O], another method was also used: the O atom titration by Br_2, leading to $[O]_0 = ([Br] + [BrO])/2$. As shown in Figure 7, the observed

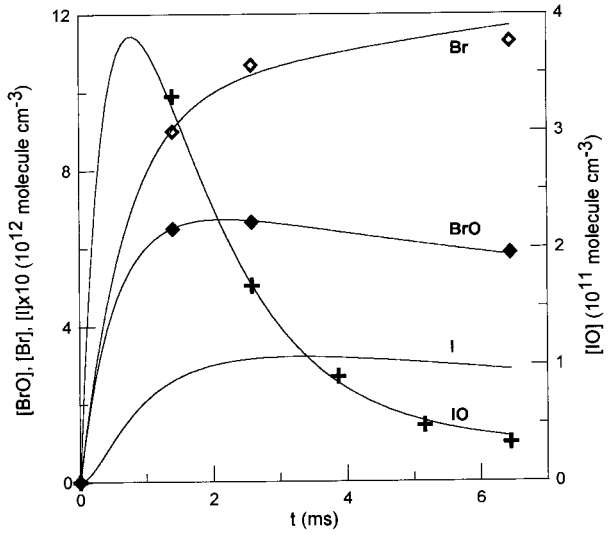

Figure 7. Reaction BrO + IO → products (1): IO kinetics in the presence of Br atoms: example of experimental (points) and simulated (solid lines) kinetics.

concentrations of Br and BrO changed only slightly on the time scale of the observations ($t > 1.5$ ms). The values of [Br] and [BrO] given in Table 3 are the corresponding mean values of the quasi-stationary concentrations.

The first five reactions in the mechanism used in the curve fitting procedure (Table 2) characterize the sources of the active species and are not important for the determination of the rate constant of IO + BrO reaction. The rate constant of reaction 3 was varied to provide the best agreement between the calculated and measured concentrations of IO, BrO, and Br at the shortest reaction times. The best-fit values of k_3 were always in the range $(3-8) \times 10^{-12}$ cm^3 molecule^{-1} s^{-1}, which agrees with the measured value $k_3 = 3.7 \times 10^{-12}$ cm^3 molecule^{-1} s^{-1}.[18] The results of the simulations were not sensitive to reactions 8 and −8, whereas the BrO + BrO reaction (13) was important only for the Br/BrO partitioning.

It was anticipated that such experiments could lead to the determination of the total rate constant of reaction 1. However, it was observed that the simulated kinetics of IO were not sensitive to the I-atom-forming channels of reaction 1. The reason for this can be easily understood from the analysis of the I atom kinetics, for example, in Figure 7, where the calculated time profile for [I] is shown (it was not possible to measure the low concentrations of I atoms, due to a significant residual signal at $m/e = 127$ (I^+), coming from the CF_3I ionization−decomposition in the ion source of the mass spectrometer). During the observation time ($t \geq 2$ ms), the I concentration remained almost unchanged and could be considered in steady state:

$$d[I]/dt = (k_{1b} + k_{1c})[IO][BrO] + k_{14}[IO][Br] + k_{19}[O][IO] - k_{-14}[I][BrO] = 0$$

Only the major processes affecting I concentration were taken into account here. All of these reactions are involved in IO formation or consumption. Their net impact on IO kinetics can be considered as negligible, because the same combination of the terms of the above expression (equal to zero) is included in the calculation of d[IO]/dt. Hence, IO decays were mainly due to the non-I-atom-producing channels of reaction 1 and the IO homogeneous and heterogeneous losses. Finally, this series of experiments provided a complementary determination of the sum

TABLE 3: Reaction IO + BrO → Products (1): IO Kinetics in the Presence of Br

$[O]_0$[b]	$[CF_3I]_0$[c]	$[Br_2]_0$[c]	[BrO][b]	[Br][b]	$k_{1a} + k_{1d}$[d] ($\pm 2\sigma$)
1.2	1.5	6.3	1.0	1.15	8.7 ± 1.1
1.8	2.9	7.6	1.4	1.7	8.4 ± 0.7
2.6	1.1	7.4	2.0	2.65	9.1 ± 1.8
4.0	1.1	6.1	2.6	4.2	7.8 ± 1.6
4.6	1.2	7.7	3.5	4.6	7.7 ± 0.9
5.2	1.1	8.2	3.8	5.5	7.9 ± 1.3
8.4	1.1	7.0	5.3	8.5	9.0 ± 1.4
9.0	0.9	6.0	5.0	10.0	7.7 ± 2.0
11.0	1.4	6.5	6.3	11.0	8.7 ± 1.7

[a] Experimental conditions and data for the non-I-atom producing channels. Units are (*b*) -10^{12} molecule cm^{-3}, (*c*) -10^{13} molecule cm^{-3}, (*d*) -10^{-11} cm^3 molecule^{-1} s^{-1}.

of the rate constants $k_{1a} + k_{1d}$. The results are given in Table 3, and the mean value derived is

$$k_{1a} + k_{1d} = (8.3 \pm 1.6) \times 10^{-11} \text{ cm}^3 \text{ molecule}^{-1} \text{ s}^{-1}$$

This value agrees quite well with that obtained in the previous section: $(7.5 \pm 1.0) \times 10^{-11}$ cm^3 molecule^{-1} s^{-1}.

As it is shown below, the IBr-forming channel (reaction 1d), which is one of the two non-I-atom-forming channels of reaction 1, is of minor importance. Therefore, the simulations were made using only channel 1a, forming Br and OIO. The reaction between Br and OIO was also introduced in the modeling calculation:

$$Br + OIO \rightarrow BrO + IO(-1a)$$

An upper limit of 3×10^{-12} cm^3 molecule^{-1} s^{-1} was found for the rate constant of this endothermic reaction (see Discussion).

(c) Branching Ratio for the Sum of Br- and IBr-Forming Channels. In this series of experiments, the consumption of BrO radicals due to their reaction with IO and the formation of IBr were observed simultaneously. BrO radicals were formed in the movable injector by the reaction of Br atoms with ozone, and IO radicals were produced by the reaction of O atoms (inlet 3) with I_2 (inlet 4). The initial concentrations of the reactants were $[BrO]_0 = (0.3-3.0) \times 10^{12}$ molecule cm^{-3} and $[IO]_0 = (1.0-5.0) \times 10^{11}$ molecule cm^{-3}. O_3 and I_2 were present at relatively high concentrations: $[O_3] = (0.8-2.0) \times 10^{15}$ molecule cm^{-3} and $[I_2] = (1-2) \times 10^{14}$ molecule cm^{-3}. In experiments performed at fixed reaction time ($t \approx 0.03$ s), both the consumption of BrO and the formation of IBr were observed. Under the conditions used, Br atoms formed either in reaction 1 or in the BrO self-reaction would have reacted with I_2 to form IBr and I atoms (converted back to IO). The formation of IBr was due either to channel 1d or to the reactions of Br with I_2, Br being formed in channels 1a and 1b and in the reaction BrO + BrO → Br + Br + O_2 (13a). The latter reaction was estimated to contribute 5−30% (depending on the experimental conditions) to the total concentration of the IBr formed. Reactions 1, 13, and the BrO wall loss were responsible for the BrO consumption in these experiments, the contribution of reaction 1 being the major one. Neglecting the contributions of BrO wall loss and reaction 13 to the BrO consumption and IBr formation, the measurement of the ratio $\Delta[IBr]/\Delta[BrO]$ can be considered as the measurement of the branching ratio for the sum of IBr- and Br-producing channels of reaction 1. The results thus obtained in a series of 13 kinetic runs are summarized in Figure 8, which shows the dependence of [IBr] produced against [BrO] con-

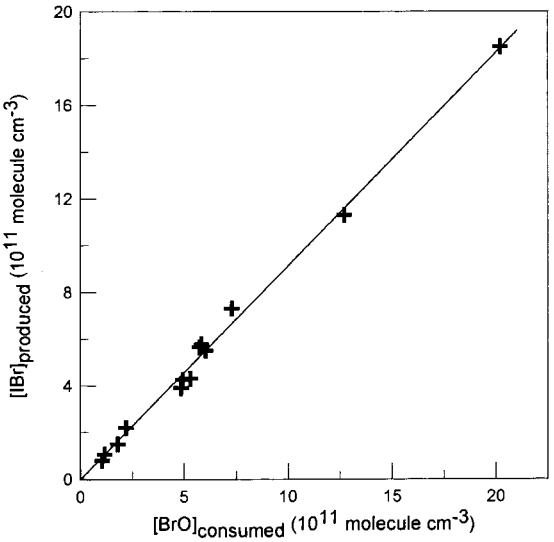

Figure 8. Reaction BrO + IO → products (1): dependence of the concentration of IBr produced on the concentration of BrO consumed in the presence of excess of I_2 and O_3 (see text).

TABLE 4: Reaction IO + BrO → Products (1): Reduced Mechanism Used in the Simulation of BrO and IBr Kinetics for the Determination of k_1

reaction	no.	rate constant[a]	ref
BrO + IO → Br (+ OIO)	1	variable	
BrO + BrO → Br + Br + O_2	13a	2.35×10^{-12}	this work
BrO + BrO → Br_2 + O_2	13b	4×10^{-13}	this work
BrO + wall → loss		0.5	this work
Br + I_2 → IBr + I	5	1.2×10^{-10}	16
Br + O_3 → BrO + O_2	10	1.2×10^{-12}	13

[a] Units are cm^3 $molecule^{-1}$ s^{-1} for bimolecular reactions and s^{-1} for heterogeneous reaction.

sumed. The linear least-squares fit to these experimental data gives

$$(k_{1a} + k_{1b} + k_{1d})/k_1 = [\mathrm{IBr}]/[\mathrm{BrO}] = 0.92 \pm 0.11$$

(the uncertainty represents 1σ + 10%).

In several studies,[27-29] a dark reaction $I_2 + O_3$ was observed, leading to the formation of IO radicals and aerosols. On the time scale of the present experiments and in the ranges of $[I_2]$ and $[O_3]$, no evidence was found for this dark reaction. However, at higher concentrations of the reactants (for $[O_3] \times [I_2] \geq 6$ times higher that that used above) IO formation was observed.

(d) Total Rate Constant of Reaction 1. In this series of experiments, conducted under the same experimental conditions as above, the kinetics of BrO decay and IBr formation were monitored. The observed BrO and IBr temporal profiles were simulated using the experimental profiles of IO and the reduced reaction mechanism, given in Table 4.

As mentioned above, the experimental profiles obtained for IO were not simulated, because additional uncertainty would have been introduced, mainly due to the reaction IO + IO, for which the channels are not well established, and also due to the IO wall loss, which was rather important due to the relatively low concentrations of BrO used in these experiments. To interpret the experimental observations, a simulation of the BrO profiles was made to extract the overall rate constant of reaction 1. A simulation of the IBr profiles was also made to determine the total rate constant for the Br- and IBr-forming channels ($k_{1a} + k_{1b} + k_{1d}$). It was observed that the difference between both calculations was <10%. This is in agreement with the results

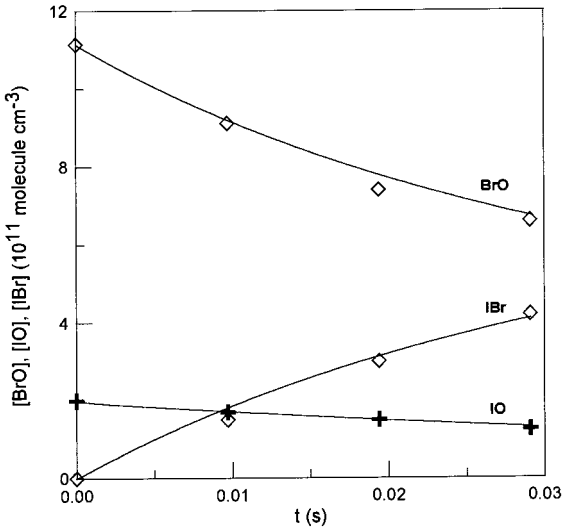

Figure 9. Reaction BrO + IO → products (1): example of experimental (points) and simulated (solid lines) kinetics for the reactants, IO and BrO, and for the reaction product IBr.

TABLE 5: Reaction IO + BrO → Products (1): Experimental Conditions and Simulated Total Rate Constant (See Text)

$[IO]_0$ (10^{11} molecule cm^{-3})	$[BrO]_0$ (10^{11} molecule cm^{-3})	k_1 ($\pm 2\sigma$) (10^{-11} cm^3 $molecule^{-1}$ s^{-1})
1.0	4.2	8.9 ± 0.3
1.5	10.0	8.9 ± 2.2
1.6	5.7	9.1 ± 0.7
2.0	11.1	8.3 ± 1.1
2.1	9.4	9.3 ± 1.1
2.7	3.3	6.7 ± 1.1
2.9	10.2	8.9 ± 1.0
4.5	9.2	9.0 ± 1.8
5.1	9.5	7.4 ± 0.6

obtained above, and this difference is lower than the experimental accuracy. Therefore, it was preferred to fit all of the data using the mechanism of Table 4 and considering $k_1 \approx k_{1a} + k_{1b} + k_{1d}$. Figure 9 shows an example of such a simulation, and all of the results are summarized in Table 5, providing the following mean value for k_1:

$$k_1 = (8.5 \pm 1.5) \times 10^{-11}\ \mathrm{cm^3\ molecule^{-1}\ s^{-1}}$$

(the uncertainty is 2σ). The simulations were not sensitive to reactions 5 and 10, because the $[I_2]/[O_3]$ ratio in the experiments was always maintained at a level high enough to totally convert Br into IBr. These simulations were also not sensitive to reactions 13 and 17.

(e) Branching Ratio for the IBr-Forming Channel (Reaction 1d). The major limitation in the determination of the branching ratios for multichannel IO reactions in discharge flow experiments comes from the fact that IO cannot be generated at relatively high concentrations. This is a consequence of the very fast self-combination of IO and also of heterogeneous effects such as an irreversible contamination of the surfaces in the presence of high concentrations of IO. This is particularly troublesome when small amounts of minor products have to be quantified. In the case of the IO + ClO reaction,[9] for example, this difficulty was overcome by using a continuous external source of IO: the I + O_3 reaction was used to regenerate the IO consumed in their reaction with ClO. As a result, relatively high steady-state IO concentrations could be reached and the formation of the different products could be measured. The

situation is more complex for the IO + BrO reaction. First, secondary reactions involving IO, BrO, and the possible products of reaction 1, I and Br, are fast:

$$IO + Br \rightarrow I + BrO \quad (14)$$

$$I + BrO \rightarrow IO + Br \quad (-14)$$

Second, the BrO self-reaction is relatively rapid compared to the ClO one and produces Br atoms, which are also expected to be produced in reaction 1.

To establish the branching ratio for the IBr-forming channel (reaction 1d), a chemical system was used, in which the two processes, the IO formation and its rapid consumption by reaction 1, occurred simultaneously. This had the advantage of forming relatively high concentrations of products and, at the same time, locally high IO concentrations could be avoided. To achieve these conditions, I_2 was initially introduced through the movable injector (inlet 2) and titrated by an excess of Br atoms (inlet 1). The corresponding concentration of I atoms formed ($[I] = 2[I_2]_0$) was measured. Subsequently, a BrO/O_3 mixture was added into the reactor, BrO being formed in the reaction of Br atoms (inlet 3) with O_3 introduced through the sidearm tube (inlet 4). Iodine atoms, coming from the injector, reacted with O_3 to produce IO radicals, which in turn reacted with BrO, giving the products of reaction 1. Thus, the initial I atoms were stoichiometrically converted to the products of reaction 1. It should be noted that I atoms can react with BrO in reaction −14. However, this reaction also leads to IO formation, which does not change the concentration of I atoms converted to the products of reaction 1. The IO consumption by reaction 7 could be considered negligible compared with that by reaction 1, due to the excess of BrO over IO (k_1 and k_7 are comparable). The following concentrations of the reactants were used: $[I]_0 = (0.4-2.0) \times 10^{12}$ molecule cm^{-3}, $[BrO] = 2 \times 10^{13}$ molecule cm^{-3}, and $[O_3] = (0.8-3.0) \times 10^{15}$ molecule cm^{-3}. As expected, a complete disappearance of I and IO was observed. Under these conditions, IBr was not detected among the products and the upper limit of the branching ratio for channel 1d could be derived: $k_{1d}/k_1 < 0.05$. In a few experiments, the reaction of excess Br with IBr (instead of I_2) was used to form I atoms. In this case, the initial concentration of I atoms was equal to $[IBr]_0$, leading to $k_{1d}/k_1 = [IBr]_{pr}/[IBr]_0$, where $[IBr]_{pr}$ was the concentration of IBr produced in reaction 1. This method allowed for the branching ratio to be taken as the ratio of the IBr signals, without any absolute calibration. The same result as above was obtained for k_{1d}/k_1. Possible reactions of IBr that might have influenced the result obtained for k_{1d}/k_1 were considered. The reaction of IBr with BrO was too slow, as it has been shown before. The possible reaction $IBr + O_3 \rightarrow$ products was also negligible due to the absence of any IBr consumption by O_3 as observed in additional experiments (by introduction of IBr into the reactor and monitoring its kinetics in the presence of ozone).

Discussion

All of the kinetic data obtained above for the IO + BrO reaction and its different channels

$$IO + BrO \rightarrow Br + OIO \quad (1a)$$

$$\rightarrow Br + I + O_2 \quad (1b)$$

$$\rightarrow I + OBrO \quad (1c)$$

$$\rightarrow IBr + O_2 \quad (1d)$$

resulting from the various experiments described in the previous part can be summarized as follows:

$$k_1 = (8.5 \pm 1.5) \times 10^{-11} \text{ cm}^3 \text{ molecule}^{-1} \text{ s}^{-1} \text{ (section d)}$$

$$k_{1a} + k_{1d} = (7.5 \pm 1.0) \times 10^{-11} \text{ cm}^3 \text{ molecule}^{-1} \text{ s}^{-1} \text{ (section a)}$$

$$k_{1a} + k_{1d} = (8.3 \pm 1.6) \times 10^{-11} \text{ cm}^3 \text{ molecule}^{-1} \text{ s}^{-1} \text{ (section b)}$$

$$(k_{1a} + k_{1b} + k_{1d})/k_1 = 0.92 \pm 0.11 \text{ (section c)}$$

$$k_{1d}/k_1 < 0.05 \text{ (section e)}$$

Analysis of these data gives branching ratios of 0.8−1.0, <0.3, and <0.05 for the formation of Br, I, and IBr, respectively. The following range or upper limits for the branching ratios for the rate constants of the individual channels of reaction 1 are as follows:

$$k_{1a}/k_1 = 0.65-1.0$$

$$k_{1b}/k_1 < 0.3$$

$$k_{1c}/k_1 < 0.2$$

$$k_{1d}/k_1 < 0.05$$

$$(k_{1b} + k_{1c})/k_1 < 0.3$$

For the total rate constant of reaction 1 the value obtained in the present study is

$$k_1 = (8.5 \pm 1.5) \times 10^{-11} \text{ cm}^3 \text{ molecule}^{-1} \text{ s}^{-1}$$

The data from this work can be compared with those of two recent studies.[11,12] In reference 11, the value of the overall rate constant was derived from the simulation of the BrO and IO experimental profiles, observed in the photolysis of $Br_2/I_2/N_2O$ mixtures. At $P = 200$ Torr and $T = 295$ K, the value obtained for k_1 was $(6.9 \pm 2.7) \times 10^{-11}$ cm^3 $molecule^{-1}$ s^{-1}. In reference 12, reaction 1 was studied at $P = (6-15)$ Torr and $T = 204-388$ K, using pulsed laser photolysis coupled to a discharge flow tube for the production of the radicals and pulsed laser-induced fluorescence and UV absorption for the detection of IO and BrO, respectively. The Arrhenius expression $k_{non-I} = (2.5 \pm 1.0) \times 10^{-11} \exp[(260 \pm 100)/T]$ cm^3 $molecule^{-1}$ s^{-1} was obtained for the rate constant of the non-I-atom-producing channels of reaction 1. This expression gives the value 6.0×10^{-11} cm^3 $molecule^{-1}$ s^{-1} at $T = 298$ K. Furthermore, from the simulation of the IO temporal profiles, Gilles et al.[12] have given an upper limit of 35% for the I-atom-producing channels, leading to an upper limit of 1.0×10^{-10} cm^3 $molecule^{-1}$ s^{-1} for the total rate constant. Considering the uncertainty ranges, all of these data are in good agreement with those obtained in the present study, that is, $k_1 = (8.5 \pm 1.5) \times 10^{-11}$ cm^3 $molecule^{-1}$ s^{-1}, with an upper limit of 30% for the branching ratio of the I-forming channels, reactions 1b and 1c. The detailed kinetic study presented in this work leads to a better evaluation of the branching ratios for the individual channels of reaction 1, which improves the understanding of the mechanism of the IO + BrO reaction.

The major channel of reaction 1 is channel 1a, which forms Br atoms and OIO radicals. The chemistry and thermochemistry of OIO are not known so far. Only spectroscopic data have appeared recently.[30] The fate of OIO in the present chemical system and its possible influence on the results obtained in this study are difficult to estimate. A weak signal has been detected at $m/e = 159$ (which can be assigned to OIO) under the conditions of the experiments performed for the determination of the IBr yield (section e). The monitoring of this signal was complicated by the presence of important signals of Br_2 at $m/e = 158$ and 160. If this signal was attributed to OIO, the observed temporal profiles would indicate a rapid formation of OIO followed by its rapid consumption. Under the experimental conditions used, OIO could have reacted with reactants present in excess, such as O_3 or BrO, or could have disappeared at the wall of the reactor. A detailed study could not be performed due to the analytical difficulties. However, it can be noted that the temporal behavior of the signal at $m/e = 159$ apparently did not depend on O_3 concentration. In a preliminary investigation of the IO + BrO reaction,[31] using the flash photolysis−UV absorption technique, OIO has been detected as a product, whereas no evidence was found for OBrO and IBr. These qualitative observations are in good agreement with the data obtained in the present study.

Information on the enthalpy of formation of OIO radicals can be extracted from the mechanistic data obtained in the present study. Taking into account the high value of the rate constant for reaction 1, its negative temperature dependence measured in another study,[12] and its major products Br and OIO formed in channel 1a, this channel can be considered to be exothermic: $\Delta H_{1a} < 0$. Therefore, using the thermochemical data (in kcal mol^{-1}) $\Delta H_f(IO) = 27.7 \pm 1.2$,[9] $\Delta H_f(BrO) = 28.6 \pm 1.4$,[16] and $\Delta H_f(Br) = 26.7$,[13] the upper limit of $\Delta H_f(OIO)$ can be obtained:

$$\Delta H^\circ_{f,298}(OIO) \leq 32.2 \text{ kcal mol}^{-1}$$

This value strongly depends on the heats of formation of IO and BrO, which are not well established so far. In the above calculation, the values derived from recent studies in this laboratory have been used.[9,16] For comparison, the values given in the most recent evaluations are (in kcal mol^{-1}) $\Delta H_f(IO) = 30.5 \pm 2$,[13] 25.6,[20] and 30.1 ± 4.3;[32] and $\Delta H_f(BrO) = 30 \pm 2$,[13] 29.9,[20] and 30.1 ± 0.6.[17] Because no experimental data on OIO thermochemistry exist in the literature, the upper limit determined here for $\Delta H^\circ_{f,298}(OIO)$ can be compared with the estimated value: $\Delta H^\circ_{f,298}(OIO) = 38 \pm 6$ kcal mol^{-1}.[32] This value was obtained from the enthalpy of atomization $\Delta_{at}H^\circ_0(OIO)$, which was extracted from the relationship $\Delta_{at}H^\circ_0(OIO) = 1.94\ D^\circ_0(IO)$ (the factor 1.94 being the ratio of the corresponding values for OClO and ClO). Taking into account the uncertainty range given in ref 32 and the existing uncertainties in the thermochemical parameters for IO, the two values are not inconsistent.

The atmospheric implications of the present kinetic data can be briefly given. As previously discussed by Solomon et al.,[6] the possible role of iodine in ozone depletion in the lower stratosphere depends on the iodine abundance and on the kinetic data of the key reactions, IO + ClO, IO + BrO, and IO + HO_2, which are the rate-limiting steps of the ozone-destroying cycles. Knowledge of the branching ratios for these reactions is also important, because not all channels lead to ozone destruction. For the interhalogen reactions, the expected channels can be written (with X = Cl, Br)

$$IO + XO \rightarrow I + X + O_2 \quad (a)$$

$$\rightarrow IX + O_2 \quad (a')$$

$$\rightarrow I + OXO \quad (b)$$

$$\rightarrow X + OIO \quad (b')$$

Channel a may proceed via one or two steps with the intermediate formation of IOO or XOO, which rapidly decomposes to I + O_2 or X + O_2, respectively. Channel a′ also produces I + X + O_2, similarly to channel a, because IX readily photolyzes under sunlit conditions. Therefore, channels a and a′ will lead to the ozone loss cycle:

$$IO + XO \rightarrow I + X + O_2$$

$$I + O_3 \rightarrow IO + O_2$$

$$X + O_3 \rightarrow XO + O_2$$

$$2O_3 \rightarrow 2O_2$$

Conversely, OBrO and OIO formed in channels b and b′, respectively, will likely generate O atom by rapid photodissociation, as already observed for OClO with a quantum yield of unity,[13] leading to null cycles, such as

$$IO + XO \rightarrow X + OIO$$

$$OIO + h\nu \rightarrow O + IO$$

$$X + O_3 \rightarrow XO + O_2$$

$$O + O_2 + M \rightarrow O_3 + M$$

$$O_3 \rightarrow O_3$$

The channel forming IOOX has not been taken into account here. This adduct could be detected neither in this work, performed at 298 K, nor in the temperature-dependent study.[12] This channel, if it exists, would lead to ozone loss in a cycle similar to that of the ClO dimer (e.g., ref 33). In the first modeling calculation of the impact of iodine chemistry on stratospheric ozone,[6] both reactions IO + XO (X = Cl or Br) were assumed to have a rate constant of 1.0×10^{-10} cm^3 molecule^{-1} s^{-1} and to proceed via the unique channel a. The new laboratory data for these reactions will change the results of such calculations, as it has been already demonstrated in previous papers.[9,12] In our study on the IO + ClO reaction (reaction 9), a simple estimation of the relative importance of the iodine-initiated ozone-depleting cycles was made, considering our experimental data, namely, (i) a lower value of the total rate constant, $(1.1 \pm 0.2) \times 10^{-11}$ cm^3 molecule^{-1} s^{-1} and (ii) branching ratios of 0.25 and 0.2 for channels a and a′, respectively. It appeared that the IO + ClO reaction contributed significantly less to the total ozone loss. The relative efficiency per atom of iodine compared to chlorine in depleting ozone, near 15−20 km, was estimated to be reduced from >1000 to ~300. The data from the present work will still reduce this relative efficiency. If the total rate constant of the IO + BrO reaction is not different from the previously estimated value, the determination of the product yields of this reaction should greatly reduce the impact on the ozone loss. The major channel, forming OIO (channel b′) with a branching ratio ranging between 0.65 and 1.0, leads to a null cycle. Therefore, if the upper limit of 0.35 is taken for the branching ratio for channels a + a′ for X = Br, the relative efficiency I/Cl of 300 estimated

above is reduced to 150 and to around 100 if the branching ratio is 10 times lower than the upper limit. Ozone destruction rates due to iodine chemistry have also been calculated in the other recent study of the IO + BrO reaction,[12] concluding that this reaction makes a significant contribution "with the caveat that the products of this reaction lead to ozone loss". The mechanistic data of the present study suggest that this contribution will be less important. Therefore, IO + HO_2 reaction should dominate in the ozone loss rate due to iodine chemistry. However, this discussion remains somewhat speculative, and a more quantitative statement requires determination of both the branching ratio of the OIO-forming channel at stratospheric temperatures and the fate of the OIO radical, although a rapid photodissociation to O and IO can be anticipated to occur by analogy with OClO and OBrO.

The reactions of IO with other radicals are also of increasing interest for tropospheric chemistry, because the IO radical has been detected in the marine boundary layer very recently.[34] Although no ClO and BrO could be detected simultaneously at the same site, that does not preclude the simultaneous presence of IO, ClO, and/or BrO radicals in the troposphere making the interhalogen reactions IO + ClO or IO + BrO of potential significance, together with the IO + HO_2 reaction,[35] and possibly with the IO + CH_3O_2 reaction, which has not been investigated so far.

Acknowledgment. This work was supported by the European Commission (Contract LEXIS, ENV4-CT95-0013).

References and Notes

(1) Chameides, W. L.; Davis, D. D. *J. Geophys. Res.* **1980**, *85*, 7383.
(2) Jenkin, M. E. In *The Tropospheric Chemistry of Ozone in the Polar Regions*; NATO ASI Series; Niki, H., Becker, K. H., Eds.; Springer-Verlag: New York, 1993; Vol. 17.
(3) Barrie, L. A.; Bottenheim, J. W.; Schnell, R. C.; Crutzen, P. J.; Rasmussen, R. A. *Nature* **1988**, *334*, 138.
(4) *Arctic Tropospheric Ozone Chemistry (ARCTOC)*; Final report of the EU project; Platt, U., Lehrer, E., Eds.; Heidelberg, 1997.
(5) Davis, D.; Crawford, J.; Liu, S.; Mckeen, S.; Bandy, A.; Thornton, D.; Rowland, F.; Blake, D. *J. Geophys. Res.* **1996**, *101*, 2135.
(6) Solomon, S.; Garcia, R. R.; Ravishankara, A. R. *J. Geophys. Res.* **1994**, *99*, 20491.
(7) Wennbegr, P. O.; Brault, J. W.; Hanisco, T. F.; Salawitch, R. J.; Mount, G. H. *J. Geophys. Res.* **1997**, *102*, 8887.
(8) Pundt, I.; Phillips, C.; Pommereau, J. P. Presented at the XVIII Quadrennial Ozone Symposium, L'Aquila, Italy, Sept 1996.
(9) Bedjanian, Yu.; Le Bras, G.; Poulet, G. *J. Phys. Chem. A* **1997**, *101*, 4088.
(10) Turnipseed, A. A.; Gilles, M. K.; Burkholder, J. B.; Ravishankara, A. R. *J. Phys. Chem. A* **1997**, *101*, 5517.
(11) Laszlo, B.; Huie, R. E.; Kurylo, M. J.; Miziolek, A. W. *J. Geophys. Res.* **1997**, *102*, 1523.
(12) Gilles, M. K.; Turnipseed, A. A.; Burkholder, J. B.; Ravishankara, A. R.; Solomon, S. *J. Phys. Chem. A* **1997**, *101*, 5526.
(13) De More, W. B.; Sander, S. P.; Golden, D. M.; Hampson, R. F.; Kurylo, M. J.; Howard, C. J.; Ravishankara, A. R.; Kolb, C. E.; Molina, M. J. *Chemical Kinetics and Photochemical Data for Use in Stratospheric Modeling*; NASA, JPL, California Institute of Technology: Pasadena, CA, 1997.
(14) Chase, M. W.; Davies, C. A.; Downey, J. R.; Frurip, D. J.; McDonald, R. A.; Syverud, A. N. *JANAF Thermochemical Tables*, 3rd ed.; NBS: Washington, DC, 1985.
(15) Bedjanian, Yu.; Le Bras, G.; Poulet, G. *Int. J. Chem. Kinet.* **1998**, in press.
(16) Bedjanian, Yu.; Le Bras, G.; Poulet, G. *Chem. Phys. Lett.* **1997**, *266*, 233.
(17) Chase, M. W. *J. Phys. Chem. Ref. Data* **1996**, *25*, 1069.
(18) Gilles, M. K.; Turnipseed, A. A.; Talukdar, R. K.; Rudich, Y.; Villalta, P. W., Huey, L. G.; Burkholder, J. B.; Ravishankara, A. R. *J. Phys. Chem.* **1996**, *100*, 14005.
(19) Harwood, M. H.; Rowley, D. M.; Cox, R. A.; Jones, R. L. *J. Phys. Chem. A* **1998**, *102*, 1790.
(20) Atkinson, R.; Baulch, D. L.; Cox, R. A.; Hampson, R. F.; Kerr, J. A.; Rossy, M. J.; Troe, J. *J. Phys. Chem. Ref. Data* **1997**, *26*, 521.
(21) Gilles, M. K.; Turnipseed, A. A.; Burkholder, J. B.; Ravishankara, A. R. *Chem. Phys. Lett.* **1997**, *272*, 75.
(22) Abbatt, J. P. D.; Toohey, D. W.; Fenter, F. F.; Stevens, P. S.; Brune, W. H.; Anderson, J. G. *J. Phys. Chem.* **1989**, *93*, 1022.
(23) Kaufman, F. *J. Phys. Chem.* **1984**, *88*, 4909.
(24) Morrero, T. R.; Mason, E. A. *J. Phys. Chem. Ref. Data* **1972**, *1*, 3.
(25) Malleson, A. M.; Kellett, H. M.; Myhill, R. G.; Sweetenham, W. P. *FACSIMILE*; AERE Harwell Publications Office: Oxfordshire, U.K., 1990.
(26) Young, M. A.; Pimentel, G. C. *Int. J. Chem. Kinet.* **1990**, *23*, 57.
(27) Cox, R. A.; Coker, G. B. *J. Phys. Chem.* **1983**, *87*, 4478.
(28) Vikis, A. C.; Macfarlan, R. *J. Phys. Chem.* **1985**, *89*, 812.
(29) Harwood, M. H.; Burkholder, J. B.; Hunter, M.; Fox, R. W.; Ravishankara, A. R. *J. Phys. Chem. A.* **1997**, *101*, 853.
(30) Himmelmann, S.; Orphal, J.; Bovensmann, H.; Richter, A.; Ladstatter-Weissenmayer, A.; Burrows, J. P. *Chem. Phys. Lett.* **1996**, *251*, 330.
(31) Rowley, D. Private communication.
(32) Chase, M. W. *J. Phys. Chem. Ref. Data* **1996**, *25*, 1297.
(33) Sander, S. P.; Friedl, R. R.; Yung, Y. L. *Science* **1989**, *245*, 1095.
(34) Alicke, B.; Hebestreit, K.; Platt, U.; Carpenter, L. J.; Sturges, W. T. *Ann. Geophys.* **1998**, *16* (Suppl. II), C716.
(35) Maguin, F.; Laverdet, G.; Le Bras, G.; Poulet, G. *J. Phys. Chem.* **1992**, *96*, 1775.